


## STUDY OF LONGITUDINAL FRACTURE IN NONLINEAR VISCOELASTIC BEAMS WHOSE THICKNESS GROWS WITH TIME

### ISTRAŽIVANJE PODUŽNOG LOMA KOD NELINEARNIH VISKOELASTIČNIH NOSAČA ČIJA DEBLJINA RASTE SA VREMENOM

Originalni naučni rad / Original scientific paper  
Rad primljen / Paper received: 12.12.2023  
<https://doi.org/10.69644/ivk-2024-03-0346>

Adresa autora / Author's address:  
University of Architecture, Civil Engineering and Geodesy,  
Department of Technical Mechanics, Sofia, Bulgaria,  
V.I. Rizov  0000-0002-0259-3984  
email: [v\\_rizov\\_fhe@uacg.bg](mailto:v_rizov_fhe@uacg.bg)

#### Keywords

- longitudinal fracture
- inhomogeneous material
- growing thickness
- beam structure

#### Abstract

The presented theoretical paper describes a study of longitudinal fracture behaviour of beam structures whose configuration changes with time. In particular, fracture in beams whose thickness grows with time is considered. The beam upper surface grows upwards at a constant rate. The configuration of the beam lower surface remains unchanged with time. The beams under consideration exhibit continuous material inhomogeneity along their thickness. Therefore, the material properties involved in the present analysis are continuous functions of the  $z$ -coordinate. The time-dependent mechanical behaviour of beams loaded in bending is treated by a nonlinear viscoelastic model. The stress-strain-time relationship of the model is derived by analysing the mechanical response of the model components (springs and dashpots) under strains increasing with time. The longitudinal fracture in the beams of growing thickness is characterised by the strain energy release rate. For this purpose, a solution of the strain energy release rate that takes into account the beam thickness growth with time is derived analytically. The  $J$  integral is used for checking of the results obtained. The effect of parameter values controlling the thickness growth on longitudinal fracture is assessed.

#### INTRODUCTION

Engineering materials with smooth inhomogeneity have a wide range of applications, and nowadays their use is quickly increasing in various spheres of engineering /1-5/. Continuous change of properties of these materials along one or more coordinates can be tailored to meet special needs such as, for example, specific distribution of strength and stiffness in a structural member /6-8/. In this way, the performance of continuously inhomogeneous (functionally graded) materials can be considerably improved which results in a constant increase of the use of these materials in a great number of applications in aerospace, aeronautics, nuclear reactors, biomedicine, microelectronics and other important sectors of up-to-date engineering, /9-13/.

Structural members made of continuously inhomogeneous engineering materials fail very often as a result of longi-

#### Ključne reči

- podužni lom
- nehomogeni materijal
- rastuća debljina
- struktura nosača

#### Izvod

U predstavljenom teorijskom radu se opisuje istraživanje podužni lom konstrukcije nosača čija se konfiguracija menja u toku vremena. Zapravo, razmatra se lom u nosačima čija se debljina povećava sa vremenom. Gornja površina nosača se razvija u smeru na gore konstantnom brzinom. Konfiguracija donje površine nosača ostaje nepromenjena u toku vremena. Razmatrani nosači pokazuju kontinualnu nehomogenost materijala u pravcu debljine. Stoga su osobine materijala u ovoj analizi oblika neprekidnih funkcija koordinate  $z$ . Vremenski zavisno mehaničko ponašanje nosača opterećenih na savijanje se razmatra primenom nelinearnog viskoelastičnog modela. Naponsko-deformacijsko-vremenska povezanost modela se izvodi analizom mehaničkog odziva komponenata modela (opruga i prigušivača) koji se deformišu u toku vremena. Podužni lom u nosačima sa rastućom debljinom karakteriše brzina oslobađanja deformacione energije. Za tu svrhu se analitički izvodi rešenje za brzinu oslobađanja deformacione energije, koje uzima u obzir razvoj debljine nosača sa vremenom. Koristi se  $J$  integral za proveru dobijenih rezultata. Data je procena uticaja veličine parametara koji upravljaju rastom debljine nosača na podužni lom.

tudinal fracture. The mainspring for this is that some continuously inhomogeneous (functionally graded) materials can be built-up layer-by-layer which results in a low tensile strength transversally to the layers, /14/. Therefore, the functioning of continuously inhomogeneous structures depends considerably on their longitudinal fracture behaviour.

This paper gives a longitudinal fracture analysis of a continuously inhomogeneous nonlinear viscoelastic beam structure whose thickness grows with time in contrast to previous publications which consider beams with time-independent dimensions /15-17/. The interest towards longitudinal fracture in beam configurations with growing thickness is provoked by the rapid development of additive-manufacturing technologies (these technologies include adding of thin layers). However, beams manufactured by layer-based approach collapse often as a result of longitudinal fracture (this is the primary motive for the present study). In this

paper, the strain energy release rate for the longitudinal crack is determined through energy balance analysis with considering the growth of the beam thickness. A check-up of the strain energy release rate is performed with the help of the J-integral method.

LONGITUDINAL FRACTURE ANALYSIS

The beam structure in Fig. 1 is continuously inhomogeneous along the thickness. A longitudinal crack of length,  $a$ , is situated in the beam (Fig. 1). The thicknesses of the lower and upper crack arms are  $h_1$  and  $h_2$ .

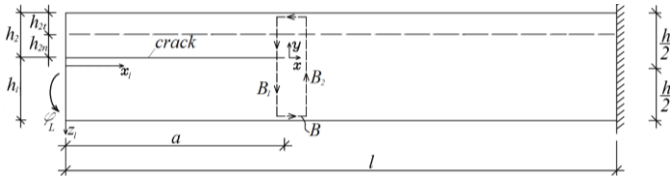


Figure 1. Inhomogeneous viscoelastic beam with longitudinal crack.

The thickness of the beam increases with time so that the upper surface of the beam grows upwards. As a result of this, the thickness of the upper crack arm grows with time,  $t$ , while the thickness of the lower crack arm does not change. The growth of the upper crack arm thickness is expressed as (Fig. 1)

$$h_2 = h_{2n} + h_{2t}, \tag{1}$$

where:  $h_{2t} = v_{h2} t$ . Here,  $v_{h2}$  is the rate. The thickness of the beam,  $h$ , is written as (Fig. 1)

$$h = h_1 + h_{2n} + v_{h2} t. \tag{2}$$

A rotation,  $\varphi_L$ , is applied at the free end of the lower crack arm (Fig. 1). The variation of  $\varphi_L$  with time is expressed as  $\varphi_L = v_{\varphi L} t$ , where  $v_{\varphi L}$  is the rate.

The beam under consideration has nonlinear viscoelastic behaviour treated by the mechanical model shown in Fig. 2.

The model is under strain,  $\varepsilon$ , that varies with time according to the following dependence:

$$\varepsilon = v_\varepsilon t, \tag{3}$$

where:  $v_\varepsilon$  is strain rate. The springs with moduli of elasticity,  $E_1$  and  $E_2$ , and the dashpots with coefficients of viscosity,  $\eta_1$  and  $\eta_2$ , have linear behaviour (Fig. 2). Nonlinear behaviour is modelled by the nonlinear dashpot, ( $nld$ ), situated as shown in Fig. 2.

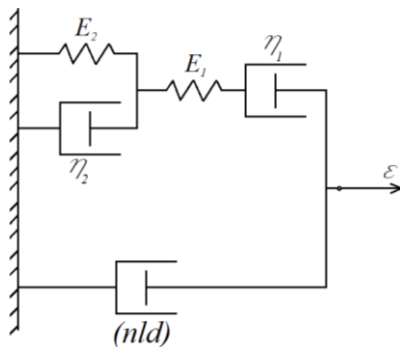


Figure 2. Nonlinear viscoelastic model.

The following constitutive law is used for describing the dependence between the stress,  $\sigma_{nld}$ , and strain rate,  $\dot{\varepsilon}$ , in the nonlinear dashpot /18, 19/:

$$\sigma_{nld} = \frac{D\dot{\varepsilon}}{\sqrt{1+g^2(\dot{\varepsilon})^2}}, \tag{4}$$

where:  $D$  and  $g$  are parameters which take into account the nonlinearity. By using of Eq.(3) and Eq.(4), one obtains

$$\sigma_{nld} = \frac{Dv_\varepsilon}{\sqrt{1+g^2v_\varepsilon^2}}. \tag{5}$$

The strain,  $\varepsilon_{E2}$ , in the linear-elastic spring with modulus of elasticity,  $E_2$ , is found from the following differential equation (Fig. 2):

$$\ddot{\varepsilon}_{E2} + \beta_1 \dot{\varepsilon}_{E2} + \beta_2 \varepsilon_{E2} = \beta_3, \tag{6}$$

where:

$$\beta_1 = \frac{E_2}{\eta_2} + \frac{E_1}{\eta_1} + \frac{E_1}{\eta_2}, \tag{7}$$

$$\beta_2 = \frac{E_1 E_2}{\eta_1 \eta_2}, \tag{8}$$

$$\beta_3 = \frac{v_\varepsilon E_1}{\eta_2}. \tag{9}$$

Equation (6) is worked-out by considering the dependences between the stresses in linear-elastic springs and dashpots of the model (Fig. 1). In Eq.(6),  $\dot{\varepsilon}_{E2}$  and  $\ddot{\varepsilon}_{E2}$  are the first and the second derivative of  $\varepsilon_{E2}$  with respect to time.

The solution of Eq.(6) is obtained as

$$\varepsilon_{E2}(t) = \frac{R\delta_2}{\delta_1 - \delta_2} e^{\delta_1 t} - \frac{R\delta_1}{\delta_1 - \delta_2} e^{\delta_2 t} + R, \tag{10}$$

where:

$$R = \frac{\beta_3}{\beta_1}, \tag{11}$$

$$\delta_1 = -0.5\beta_1 + \zeta, \tag{12}$$

$$\delta_2 = -0.5\beta_1 - \zeta, \tag{13}$$

$$\zeta = 0.5(\beta_1^2 - 4\beta_2)^{0.5}. \tag{14}$$

By substituting Eq.(10) in the Hook's law, one derives the following expression for the stress in the spring with modulus of elasticity,  $E_2$ :

$$\sigma_{E2}(t) = E_2 \left[ \frac{R\delta_2}{\delta_1 - \delta_2} e^{\delta_1 t} - \frac{R\delta_1}{\delta_1 - \delta_2} e^{\delta_2 t} + R \right]. \tag{15}$$

By combining the dependence,  $\sigma_{\eta_2} = \eta_2 \dot{\varepsilon}_{E2}$ , and Eq.(15), the stress in the dashpot with coefficients of viscosity,  $\eta_2$ , is obtained as

$$\sigma_{\eta_2}(t) = \eta_2 \left[ \frac{R\delta_1 \delta_2}{\delta_1 - \delta_2} e^{\delta_1 t} - \frac{R\delta_1 \delta_2}{\delta_1 - \delta_2} e^{\delta_2 t} \right]. \tag{16}$$

The stress,  $\sigma$ , in the model (Fig. 2) is found as

$$\sigma = \sigma_{E2} + \sigma_{\eta_2} + \sigma_{nld}. \tag{17}$$

From Eqs. (5), (14), (15), and (16), it follows that

$$\sigma = E_2 \left[ \frac{R\delta_2}{\delta_1 - \delta_2} e^{\delta_1 t} - \frac{R\delta_1}{\delta_1 - \delta_2} e^{\delta_2 t} + R \right] + \eta_2 \left[ \frac{R\delta_1 \delta_2}{\delta_1 - \delta_2} e^{\delta_1 t} - \frac{R\delta_1 \delta_2}{\delta_1 - \delta_2} e^{\delta_2 t} \right] + \frac{Dv_\varepsilon}{\sqrt{1+g^2v_\varepsilon^2}}. \tag{18}$$

Equation (18) is used as constitutive law for treating the mechanical behaviour of the beam in Fig. 1. The distributions of  $E_1$ ,  $E_2$ ,  $\eta_1$ ,  $\eta_2$ ,  $D$  and  $g$  along the beam thickness are presented in the form of exponential functions:

$$E_1 = E_{1up} e^{\rho_1 \frac{h+z_1}{2h}} \quad (19), \quad E_2 = E_{2up} e^{\rho_2 \frac{h+z_1}{2h}} \quad (20),$$

$$\eta_1 = \eta_{1up} e^{\rho_3 \frac{h+z_1}{2h}} \quad (21), \quad \eta_2 = \eta_{2up} e^{\rho_4 \frac{h+z_1}{2h}} \quad (22),$$

$$D = D_{up} e^{\rho_5 \frac{h+z_1}{2h}} \quad (23), \quad g = g_{up} e^{\rho_6 \frac{h+z_1}{2h}} \quad (24),$$

$$-\frac{h}{2} \leq z_1 \leq \frac{h}{2} \quad (25),$$

where:  $z_1$  is the vertical centric axis of the beam cross-section;  $E_{1up}$ ,  $E_{2up}$ ,  $\eta_{1up}$ ,  $\eta_{2up}$ ,  $D_{up}$ , and  $g_{up}$  are the values of  $E_1$ ,  $E_2$ ,  $\eta_1$ ,  $\eta_2$ ,  $D$  and  $g$  at the upper surface of the beam;  $\rho_i$  ( $i = 1, 2, \dots, 6$ ) are parameters governing the distributions.

The curvatures and the coordinates of the neutral axis of the lower crack arm (upper crack arm is free of stresses) and the un-cracked part of the beam,  $a \leq x_1 \leq l$ , used when obtaining the strain energy release rate for the crack, are determined from the equations of equilibrium

$$b \int_{-h_1/2}^{h_1/2} \sigma dz_2 = 0 \quad (26), \quad b \int_{-h_1/2}^{h_1/2} \sigma_{unc} dz_3 = 0 \quad (27),$$

$$b \int_{-h_1/2}^{h_1/2} \sigma dz_2 = b \int_{-h_1/2}^{h_1/2} \sigma_{unc} dz_3, \quad (28)$$

$$\phi_L = \kappa_1 a + \kappa_2 (l - a), \quad (29)$$

where:  $b$  is beam width;  $\sigma_{unc}$  is stress in the un-cracked part of the beam;  $z_2$  and  $z_3$  are vertical centric axes of the cross-sections of lower crack arm and un-cracked part of beam;  $l$  is beam length;  $\kappa_1$  and  $\kappa_2$  are curvatures of the lower crack arm and un-cracked part of beam. It should be specified that  $h$  is a function of time (refer to Eq.(2)).

The strain energy release rate,  $G$ , for the crack in Fig. 1 is written as

$$G = \frac{M_L}{b} \frac{\partial \phi_L}{\partial a} - \frac{1}{b} \frac{\partial U}{\partial a}, \quad (30)$$

where:  $M_L$  and  $U$  are the bending moment at the free end of the lower crack arm and strain energy in the beam, respectively. Equation (30) is found by analysing the energy balance. The quantities,  $M_L$  and  $U$ , are determined as

$$M_L = b \int_{-h_1/2}^{h_1/2} \sigma z_2 dz_2, \quad (31)$$

$$U = ab \int_{-h_1/2}^{h_1/2} u_{01} dz_2 + (l - a) b \int_{-h_1/2}^{h_1/2} u_{02} dz_3, \quad (32)$$

where:  $u_{01}$  and  $u_{02}$  are strain energy densities in the lower crack arm and un-cracked part of the beam, respectively.

The method of the J-integral is applied for check-up of the strain energy release rate [20]. The J-integral is expressed as

$$J = \int_{B_1} \left[ u_{01} \cos \alpha_{B_1} - \left( p_{x_{B_1}} \frac{\partial u}{\partial x} + p_{y_{B_1}} \frac{\partial v}{\partial x} \right) \right] ds_{B_1} + \int_{B_2} \left[ u_{02} \cos \alpha_{B_2} - \left( p_{x_{B_2}} \frac{\partial u}{\partial x} + p_{y_{B_2}} \frac{\partial v}{\partial x} \right) \right] ds_{B_2}, \quad (33)$$

where:  $B_1$  and  $B_2$  are parts of the integration contour,  $B$ , shown in Fig. 1.

MatLab<sup>®</sup> is used to perform integration in Eq.(33). The J-integral values match the strain energy release rates. This fact is a confirmation for the correctness of the strain energy release rate.

## NUMERICAL RESULTS

Numerical results are presented in this section.

The data used to obtain numerical results are as follows:  $b = 0.025$  m,  $h_1 = 0.010$  m,  $h_{2n} = 0.005$  m,  $l = 0.600$  m,  $v_{h2} = 2 \times 10^{-7}$  m/sec, and  $v_{\varphi L} = 3 \times 10^{-9}$  rad/sec. Numerical results are presented in the form of graphics in the next six figures.

The normalised strain energy release rate,  $G_N = G/(E_{1up} b)$ , is plotted in Fig. 3 for parameter  $\rho_1$ , variable at three values of parameter  $\rho_3$ .

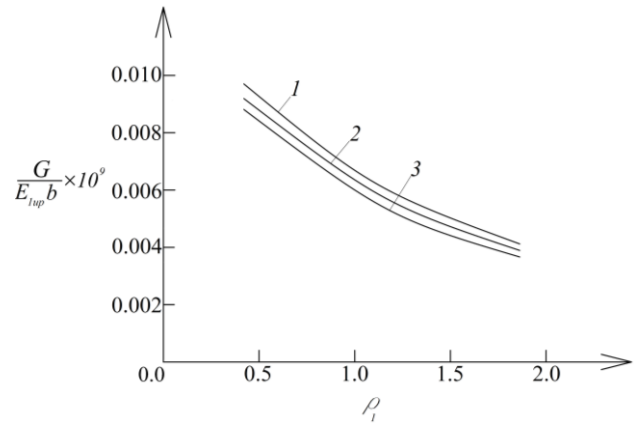


Figure 3. Plots of normalised strain energy release rate -  $\rho_1$  (curve 1 at  $\rho_3 = 0.5$ , curve 2 at  $\rho_3 = 1.0$ , and curve 3 at  $\rho_3 = 2.0$ ).

Figure 3 shows that increase of  $\rho_1$  causes a gradual reduction of strain energy release rate. Inspection of Fig. 3 indicates that variation of  $\rho_3$  in the same interval as  $\rho_1$ , i.e.,  $0.5 \leq \rho_3 \leq 2.0$ , results in a relatively modest variation of the strain energy release rate.

Plots of the normalised strain energy release rate -  $v_{h2}$  in Fig. 4 show that strain energy release rate reduces when  $v_{h2}$  grows. It is seen also in Fig. 4 that the dependence of the strain energy release rate on parameter  $\rho_4$ , has the same character, i.e., growth of  $\rho_4$  causes reduction of the strain energy release rate.

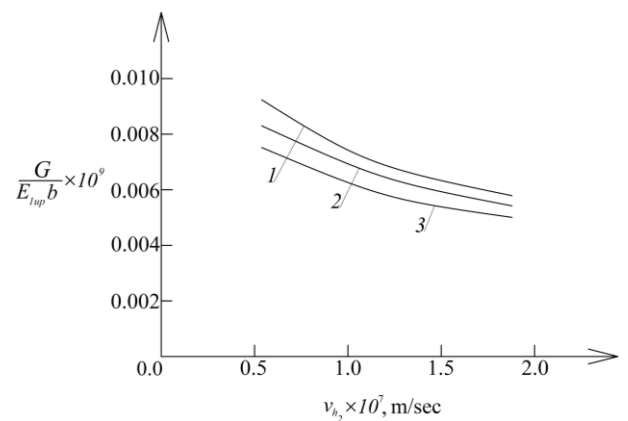


Figure 4. Plots of normalised strain energy release rate -  $v_{h2}$  (curve 1 at  $\rho_4 = 0.5$ , curve 2 at  $\rho_4 = 1.0$ , and curve 3 at  $\rho_4 = 2.0$ ).

In Fig. 5, the normalised strain energy release rate is plotted as a function of  $\rho_5$  at three values of  $v_{\varphi L}$ .

The reduction of strain energy release rate induced by growth of  $\rho_5$  is relatively modest (Fig. 5). The graphics in Fig. 5 indicate also that increase of  $v_{\varphi L}$  results in a sizable growth of the strain energy release rate.

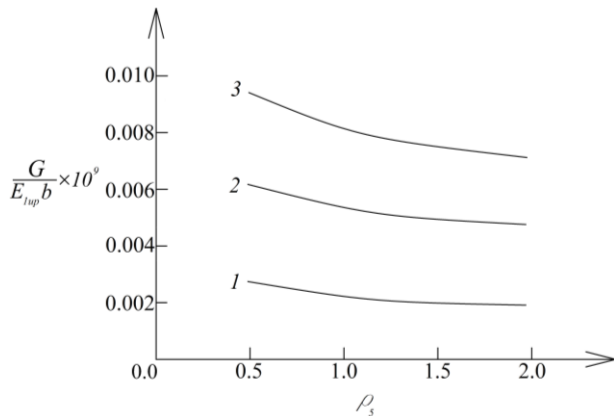


Figure 5. Plot of normalised strain energy release rate -  $\rho_5$  (curve 1 at  $v_{\phi L} = 1 \times 10^{-9}$  rad/sec, curve 2 at  $v_{\phi L} = 2 \times 10^{-9}$  rad/sec, and curve 3 at  $v_{\phi L} = 3 \times 10^{-9}$  rad/sec).

The variation of the normalised strain energy release rate with increase of  $\rho_2$  and  $h_{2n}/h_1$  ratio is illustrated by graphs plotted in Fig. 6. It can be seen in Fig. 6 that the effect of both  $\rho_2$  and  $h_{2n}/h_1$  is characterised by quick reduction of the strain energy release rate.

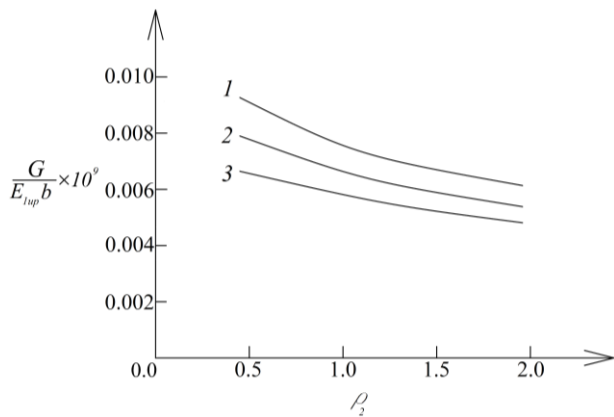


Figure 6. Plots of normalised strain energy release rate -  $\rho_2$  (curve 1 at  $h_{2n}/h_1 = 0.3$ , curve 2 at  $h_{2n}/h_1 = 0.5$ , and curve 3 at  $h_{2n}/h_1 = 0.7$ ).

Data for the influence of  $E_{2up}/E_{1up}$  and  $\eta_{2up}/\eta_{1up}$  ratios on normalised strain energy release rate are shown in Fig. 7. One can observe in Fig. 7 that  $E_{2up}/E_{1up}$  ratio has a stronger influence on strain energy release rate than that of  $\eta_{2up}/\eta_{1up}$ .

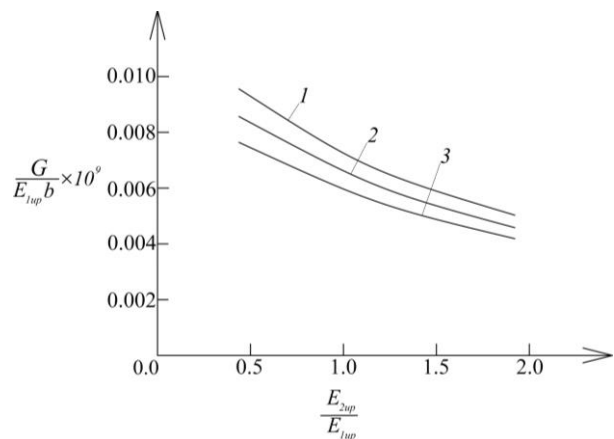


Figure 7. Plots of normalised strain energy release rate -  $E_{2up}/E_{1up}$  (curve 1 at  $\eta_{2up}/\eta_{1up} = 0.5$ , curve 2 at  $\eta_{2up}/\eta_{1up} = 1.0$ , and curve 3 at  $\eta_{2up}/\eta_{1up} = 1.5$ ).

Changes in normalised strain energy release rate induced by  $\rho_6$  and  $h_1/b$  ratio are also analysed. The results of this analysis are shown in Fig. 8. As one can see, increase of  $\rho_6$  results in growth of the strain energy release rate (Fig. 8). Rise of  $h_1/b$  ratio, however, generates reduction of strain energy release rate.

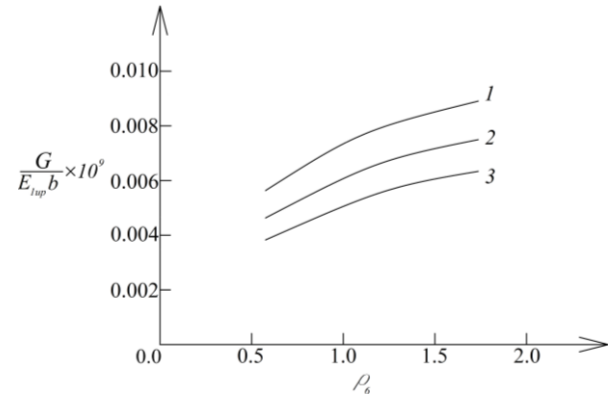


Figure 8. Plots of normalised strain energy release rate -  $\rho_6$  (curve 1 at  $h_1/b = 0.4$ , curve 2 at  $h_1/b = 0.5$ , and curve 3 at  $h_1/b = 0.6$ ).

## CONCLUSIONS

A longitudinal fracture analysis of an inhomogeneous viscoelastic beam structure whose thickness grows with time is carried-out. It is assumed that the upper surface of the beam grows upwards so that the thickness of the upper crack arm increases with time while the thickness of the lower crack arm does not change. The mechanical behaviour of the beam under increasing with time angle of rotation of the free end of the lower crack arm is described by a nonlinear viscoelastic model. The constitutive law used for treating the beam is obtained for the case when the model is under strain that increases with time. The strain energy release rate determined through the energy balance analysis is checked by method of the J-integral. Based upon the results obtained in this paper, the following conclusions can be drawn.

- The reduction of the strain energy release rate caused by increase of  $\rho_3$  and  $\rho_5$  is relatively modest in comparison with that caused by increase of  $\rho_1$ .
- The strain energy release rate reduces gradually when parameters  $v_{h2}$  and  $\rho_4$ , grow.
- Increase of  $v_{\phi L}$  results in a sizeable growth of strain energy release rate.
- Rise of  $h_{2n}/h_1$ ,  $E_{2up}/E_{1up}$ ,  $\eta_{2up}/\eta_{1up}$ , and  $h_1/b$  ratios induces reduction of strain energy release rate.
- Growth of  $\rho_6$  causes increase of strain energy release rate.

## REFERENCES

1. Dias, C.M.R., Savastano, Jr.H., John, V.M. (2010), *Exploring the potential of functionally graded materials concept for the development of fiber cement*, Constr. Build. Mater. 24(2): 140-146. doi: 10.1016/j.conbuildmat.2008.01.017
2. Fanani, E.W.A., Surojo, E., Prabowo, A.R., Akbar, H.I. (2021), *Recent progress in hybrid aluminum composite: manufacturing and application*, Metals, 11(12): 1919-1929. doi: 10.3390/met1121919
3. Radhika, N., Sasikumar, J., Sylesh, J.L., Kishore, R. (2020), *Dry reciprocating wear and frictional behaviour of B4C reinforced functionally graded and homogenous aluminium matrix com-*

- posites, *J Mater. Res. Technol.* 9(2): 1578-1592. doi: 10.1016/j.jmrt.2019.11.084
4. Udupa, G., Rao, S.S., Gangadharan, K.V. (2014), *Functionally graded composite materials: An overview*. *Proc. Mater. Sci.* 5: 1291-1299. doi: 10.1016/j.mspro.2014.07.442
  5. Hirai, T., Chen, L. (1999), *Recent and prospective development of functionally graded materials in Japan*, *Mater. Sci. Forum*, 308-311: 509-514. doi: 10.4028/www.scientific.net/MSF.308-311.509
  6. Hedia, H.S., Aldousari, S.M., Abdellatif, A.K., Fouda, N. (2014), *A new design of cemented stem using functionally graded materials (FGM)*. *Biomed. Mater. Eng.* 24(3): 1575-1588. doi: 10.233/BME-140962
  7. Nikbakht, S., Kamarian, S., Shakeri, M. (2019), *A review on optimization of composite structures Part II: Functionally graded materials*, *Compos. Struct.* 214: 83-102. doi: 10.1016/j.compstr.2019.01.105
  8. Gasik, M.M. (2010), *Functionally Graded Materials: bulk processing techniques*, *Int. J Mater. Prod. Technol.* 39(1-2): 20-29. doi: 10.1504/IJMPT.2010.034257
  9. Suresh, S., Mortensen, A., *Fundamentals of Functionally Graded Materials: Processing and Thermomechanical Behavior of Graded Metals and Metal-Ceramic Composites*, IOM Communications Ltd., London, 1998.
  10. Toudehdeghan, A., Lim, J.W., Foo, K.E., et al. (2017), *A brief review of functionally graded materials*, *MATEC Web Conf.* 131: 03010. doi: 10.1051/mateconf/201713103010
  11. Oza, M.J., Schell, K.G., Bucharsky, E.C., et al. (2021), *Developing a hybrid Al-SiC-graphite functionally graded composite material for optimum composition and mechanical properties*, *Mater. Sci. Eng.: A*, 805: 140625. doi: 10.1016/j.msea.2020.140625
  12. Yan, W., Ge, W., Smith, J., et al. (2016), *Multi-scale modeling of electron-beam melting of functionally graded materials*, *Acta Mater.* 115: 403-412. doi: 10.1016/j.actamat.2016.06.022
  13. Saiyathibrahim, A., Subramanian, R., Dhanapal, P. (2016), *Centrifugally cast functionally graded materials - A review*. In: *Proc. Int. Conf. on Systems, Science, Control, Communications, Eng. and Technol.*, vol.02: 68-73. ISBN 978-81-929866-6-1
  14. Mahamood, R.M., Akinlabi, E.T., *Functionally Graded Materials*, Springer Cham, 2017. doi: 10.1007/978-3-319-53756-6
  15. Rizov, V.I. (2018), *Delamination in multi-layered functionally graded beams - an analytical study by using the Ramberg-Osgood equation*. *Struct. Integr. Life*, 18(1): 70-76.
  16. Rizov, V.I. (2020), *Analysis of two lengthwise cracks in a viscoelastic inhomogeneous beam structure*, *Eng. Trans.* 68(4): 397-415. doi: 10.24423/EngTrans.1214.20201125
  17. Rizov, V.I. (2021), *Inhomogeneous structural component with two lengthwise cracks - a nonlinear fracture analysis*, *Struct. Integr. Life*, 21(2): 157-162.
  18. Kishkilov, M., Apostolov, R., *Introduction to Theory of Plasticity*, UACEG, Sofia, 1994.
  19. Lukash, P.A., *Fundamentals of Nonlinear Structural Mechanics*, Stroiizdat, Moscow, 1978. (in Russian)
  20. Broek, D., *Elementary Engineering Fracture Mechanics*, 2<sup>nd</sup> Ed., Springer Dordrecht, 1986. ISBN 978-90-247-2656-1

© 2024 The Author. Structural Integrity and Life. Published by DIVK (The Society for Structural Integrity and Life 'Prof. Dr Stojan Sedmak') (<http://divk.inovacionicentar.rs/ivk/home.html>). This is an open access article distributed under the terms and conditions of the Creative Commons Attribution-NonCommercial-NoDerivatives 4.0 International License